

Received April 25, 2022, accepted May 12, 2022, date of publication May 17, 2022, date of current version May 27, 2022.

Digital Object Identifier 10.1109/ACCESS.2022.3175872

# Multimode Inverter Control Strategy for LVRT and HVRT Capability Enhancement in Grid Connected Solar PV System

C. NITHYA, (Member, IEEE), AND J. PREETHA ROSELYN<sup>ID</sup>, (Senior Member, IEEE)

SRM Institute of Science and Technology, Tamil Nadu 603203, India

Corresponding author: J. Preetha Roselyn (preethaj@srmist.edu.in)

This work was supported in part by the Department of Science and Technology-Science and Engineering Research Board (DST-SERB), New Delhi, through the Project Optimal Energy Management System in Shipboard Microgrid With Solar Photovoltaic (PV), under Grant TAR/2018/000412; and in part by the National Institute of Ocean Technology for extending their support in providing research facilities.

**ABSTRACT** Grid Connected Photo Voltaic (GCPV) system should be susceptible to grid faults and load curtailment without disconnection and supports in grid stability. During grid faults, there is an increase in dc link voltage, dip in grid voltage which leads to over-current on the grid side. Similarly, when demand is suddenly removed, the voltage at the PCC rises above its nominal value. This leads to possible damage in the PV inverters and hence need to disconnection of GCPV system leading to islanding scenarios. Hence, the GCPV system need to be equipped with Fault Ride Through (FRT) capability to address the issues related to low voltage and high voltage conditions in the grid side. In this work, multimode inverter control strategy is proposed with FRT capability according to grid code compliance. An improved current control technique is proposed as FRT based protection strategy during grid faults and sudden removal of load. According to severity of faults, a fault level detection is developed which triggers the control strategies to generate the reference real and reactive power with respect to the grid code compliance. The performance analysis of the proposed FRT control strategy is implemented in 100 kW two-stage GCPV system in MATLAB/Simulink 2018b environment and tested under low voltage and high voltage ride through conditions. The proposed control strategy is implemented in hardware setup of 1 kW GCPV system. The experimental results prove the effectiveness of the proposed inverter FRT based control strategy in enhancing the system parameters during system disturbances under different modes of operation.

**INDEX TERMS** Fault ride through capability, FRT detection, grid connected solar PV, inverter control.

## NOMENCLATURE

$P$	Real power (pu).	$v_q$	quadrature axis inverter output voltage (pu).
$Q$	reactive power (pu).	$i_d$	direct axis component of grid current (pu).
$I_{pv,mppt}$	Solar PV current in MPPT mode of operation.	$i_q$	quadrature axis component of grid current (pu).
$I_{pv}^*$	Solar PV current during FRT mode of operation.	$I_d$	active current generated from LVRT grid code (pu).
$V_g$	Grid voltage level index (pu).	$I_q$	reactive current generated from LVRT grid code (pu).
$V_{gn}$	Nominal grid voltage (kV).	$I_d^*$	direct axis reference current (pu).
$V_{dc}$	DC link voltage.	$I_q^*$	quadrature axis reference current (pu).
$V_{dc}^*$	DC link voltage reference.	$V_d^*$	direct axis reference output voltage (pu).
$k_p$	Proportional component.	$V_q^*$	quadrature axis reference output voltage (pu).
$k_i$	Integral component.	$L$	inductor value (mH).
$v_d$	direct axis inverter output voltage (pu).	$P_{max}$	Maximum active power rating of the inverter during LVRT mode.

The associate editor coordinating the review of this manuscript and approving it for publication was Ying Xu<sup>ID</sup>.

$Q_{max}$	Maximum reactive power rating of the inverter during LVRT mode.
$P_{max}^*$	Maximum active power rating of the inverter during HVRT mode.
$Q_{max}^*$	Maximum reactive power rating of the inverter during HVRT mode.
$S_{max}$	Maximum apparent power rating of the inverter.
$P_{switchover}$	active power output during fault condition.
$T$	Switchover period.
$P_{LVRT}$	active power output during LVRT mode of operation.
$D$	duty cycle input to boost converter switch (%).
$K$	voltage sag level.
$I_{max}$	maximum current rating of the inverter.

**I. INTRODUCTION**

Due to increased penetration of solar power generation into the grid, disconnecting the PV plant during grid faults leads to more grid instability leading to blackouts. The essential requirement to resolve such problems is the Low Voltage Ride Through (LVRT) capability, which has to be incorporated in the PV inverter to make the GCPV stay connected to the grid in the event of grid failure. As the GCPV is unable to deliver the maximum output power during a grid failure, the inverter current increases and voltage at the PCC drops. In addition, output of the boost converter is reduced and dc link voltage across the dc capacitor shoots up to a high value. Similarly, the voltage at the PCC rises above the nominal value, during conditions like sudden disconnection of the demand. This abnormal condition makes the PV system to get disconnected from the utility grid and hence High Voltage Ride Through (HVRT) capability is required in the GCPV system. According to the recent grid code standards, during periods of low voltage at the PCC, the reactive power should be fed to the grid and during voltage rise at the PCC, reactive power should be absorbed from the grid, thereby ensuring safer limits of system parameters. Hence, the grid connected PV system with appropriate LVRT and HVRT capabilities makes the system remain connected to the grid even under abnormal conditions, which ensures system stability [1]–[4].

The Indian grid code requirement proposed for voltage dip and voltage rise at the PCC is shown in Figure 1 which satisfies IEEE 1547 standards. Figure 1 (a) represents the LVRT capability curve for Indian grid code [5], and it is clear that if the voltage dip in the grid side is below 0.15 pu, the PV system should recover to 85% of its nominal value within 3000 ms and the PV remains connected with the grid. If the system fails to recover to its nominal value within 300 ms after which the PV system is cut off from the grid. Figure 1 (b) represents the HVRT capability curve, which indicates that when the voltage at PCC is above 1.3 pu, the PV system should get back to its nominal value within 200 ms otherwise the PV system is disconnected from the grid. The tripping time for generating

**TABLE 1. Fault clearing time for LVRT and HVRT conditions.**

System Response for LVRT		System Response for HVRT	
Voltage Range (pu)	Clearing Time (secs)	Voltage Range (pu)	Clearing Time (secs)
$\frac{V_g}{V_{gn}} < 0.15$	3000	$1.1 < \frac{V_g}{V_{gn}} < 1.2$	2
$0.15 \leq \frac{V_g}{V_{gn}} \leq 0.85$	300	$1.2 < \frac{V_g}{V_{gn}} < 1.3$	0.2
$0.85 < \frac{V_g}{V_{gn}}$	0	$\frac{V_g}{V_{gn}} > 1.3$	0

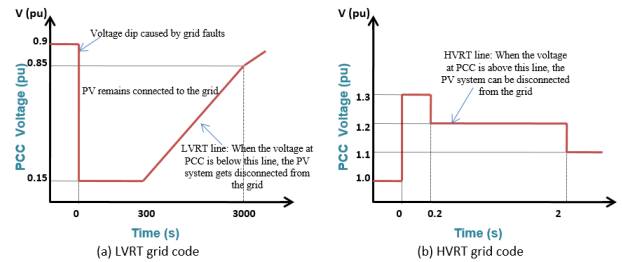


**FIGURE 1. Grid code requirement under FRT mode of operation.**

units under different level of voltage at PCC, is provided in Table 1 [5].

Many intelligent techniques have been proposed in literatures in order to overcome the drawbacks of conventional FRT controllers, such as high over currents, high dc link voltage resulting in high power losses, incorrect setting of the reference axis current during fault and insufficient reduction of grid side over currents during grid faults. A fuzzy based FRT scheme for active power injection according to the level of voltage dip at PCC has been proposed in [6]. Although this method is verified for fault conditions, it does not perform as expected in terms of regulating the DC link voltage. Ronald et al [7] discussed FRT control strategy based on fault detection scheme which provides reactive current injection by limiting active current. But the drawback is that it always injects more reactive power with active power curtailment even during less severe faults. A Fuzzy Logic based FRT controller for the operation of the inverter under normal and faulty conditions has been discussed in [8]. Furthermore, the active power is derated to zero as the voltage dip is increased and reactive power is injected into the grid for grid stability. Shetwi et al [9] suggested limiting the inverter output voltage by limiting the inductor current using hybrid reference frames. A current limiting controller strategy delivering active and reactive power depending on grid requirements is presented in [10]. This method has huge switching transients during the grid voltage recovery period. Eyad et al [11] proposed two PI regulators to regulate the active and reactive power separately when a voltage dip is detected. The proposed method performs better but additional controllers are needed to enhance the transient stability of the GCPV system.

Vivek et al [12] has implemented two dc-link regulators with different references to operate under normal and FRT modes of operation. In [13] the author has proposed an adaptive P-norm based control for the dc-dc boost converter and grid side inverter to enhance the LVRT capability of the GCPV system during grid faults. This paper shows that the maximum active current injected during a grid fault results in high grid side over currents.

Jaume *et al.* [14] discussed a series dynamic braking resistor to limit dc link overvoltage during grid failure but does not focus on the other system parameters, including grid side over current and voltage dip mitigation. Sadeghkhan *et al.* [15] presented an inverter fed microgrid in which current limiting strategy and anti-windup strategy are applied for current and voltage control respectively. As a result, currents and voltages does not exceed the threshold during fault conditions. A smooth transition in switch over operations is achieved but the control of power is not fully addressed. In the existing works, the enhancement of all system parameters is not addressed. Moreover, the FRT control strategies are not validated in real time hardware setup. In this work, the development of FRT controllers has, concentrated on both LVRT and HVRT capabilities. The double loop control is proposed with an inner and outer control loop in which inner loop consists of feed-forward decoupling strategy to decouple the real and reactive power and outer loop which limits the inverter current within safety limits. This work proposes a hybrid improved current based inverter control strategy to utilize the capacity of the PV inverter. Accordingly, the proposed system is capable of working in 3 modes: MPPT mode under normal grid conditions, LVRT mode under grid fault conditions, and HVRT mode under sudden loss of demand conditions. The system switches to LVRT mode of operation during grid faults and HVRT mode when demand loss is huge.

Joshi et al [16] provided the review of different LVRT control schemes and proposed flexible current limitation FRT strategy according to the requirements of different grid codes. The three control schemes for LVRT enhancement over a wide range of operating modes are proposed in [17]. The control scheme includes the determination of the set point of the positive sequence current, reactive power injection, and PV array output power regulation by a current limiter. In [18], selective harmonic elimination pulse width modulation optimized by genetic algorithm and an adaptive fuzzy logic-based PID controller is proposed for LVRT and HVRT control scheme. This paper avoids the fluctuations caused by sudden changes in grid voltage magnitude and turbine turbulence effects on the generator side. M. A. Khan et al [19] proposed an active and reactive power control with the dynamic voltage support for achieving LVRT capability of the grid connected PV system. The only disadvantage of this system is the overshoot and undershoot in the active power during the fault incidence. This paper discusses the importance of reactive power for a large scale PV system integration into a power distribution grid. In [20], a coordinated control algorithm that combines the reactive power capabilities of PV inverter and

STATCOM for reactive power compensation are developed. This work efficiently regulates the bus voltages during over and under-voltage conditions. In terms of reactive power control during grid faults, all the system parameters improvement are not analyzed.

**The novelty and contribution of the paper are as follows:**

- A multi-mode operation using the proposed inverter control for effective operation of the inverter during normal grid faults and demand loss.
- A voltage based FRT detection scheme is proposed to detect the voltage dip or rise and activate the LVRT and HVRT modes accordingly.
- A hybrid improved current based converter control strategy is proposed to achieve effective control over the inverter to works in all modes of operation.
- The proposed FRT scheme is also combined with a dc chopper circuit and SDBR, which significantly improves the FRT capability of the system.
- The proposed model provides increased system performance in terms of system parameters under all disturbance conditions.
- The proposed control strategy is tested in 100 kW GCPV system in MATLAB 2018b simulation platform and validated in real time hardware setup of 1 kW GCPV system.

The paper is organized as follows: Section 2 describes the proposed framework for multimode operation of inverters. Section 2.1 explains the voltage based FRT detection scheme for the grid connected PV system. Section 2.2 describes the converter control strategies under MPPT mode of operation. Section 2.3 provides the operation of control strategy under LVRT mode of operation. Section 2.4 discusses the control strategy under HVRT mode of operation. The results and discussion are provided in section 3. The conclusion and the future scope of the work are provided in section 4.

## II. PROPOSED FRAMEWORK OF MULTIMODE INVERTERS CONTROL STRATEGIES

The proposed inverter control strategy operates in a unified manner to work under multimode operations namely MPPT, LVRT and HVRT modes. When the system is under normal condition, MPPT mode is activated and when the system is subjected to disturbances, FRT mode is activated. In addition, the FRT mode is classified into LVRT and HVRT modes based on the voltage level at PCC using the proposed voltage detection scheme. The system parameters which are affected due to system disturbances are: voltage at PCC, inverter current, dc link voltage, real and reactive powers. In the proposed system, a voltage-based FRT activation scheme is developed to detect the voltage dip or rise and activate the LVRT and HVRT modes accordingly. During grid faults, it is observed that there is a voltage dip at the PCC and the system is switched to LVRT mode of operation. The system parameters get affected during grid faults in the following

**TABLE 2. Severity of fault based voltage level and clearing time.**

Severity of Fault	Voltage Level index	Tripping time (Secs)
Less severe	$0.85 < \frac{V_g}{V_{gn}} \leq 1.1$	Stay connected
Moderate severe	$0.15 \leq \frac{V_g}{V_{gn}} \leq 0.85$	3000
High severe	$\frac{V_g}{V_{gn}} < 0.15$	300

ways: high overshoot in the inverter current, voltage dip at the PCC and overshoot in dc link voltage. The proposed strategy overcomes these issues by injecting reactive power into the grid and thereby regulates the system parameters. The dc link voltage and inverter current are brought back to its nominal value by incorporating a DC chopper at the dc side and a series dynamic braking resistor at the ac side in addition to LVRT control strategy in the grid connected PV system. The HVRT mode of operation is activated when the voltage at the PCC increases above the nominal value, which occurs mainly due to sudden disconnection of the large load. The system parameters get disturbed in the following ways: voltage rise at PCC, drop in the inverter current and dc link voltage drops below the nominal value. The proposed HVRT control strategy ensure that the PV system absorbs reactive power depending on the capability of the PV inverter while maintaining the active power transfer and also limits the voltage at the PCC within the specified range.

**A. VOLTAGE BASED FRT DETECTION SCHEME**

In this work, a voltage-based FRT detection scheme is utilized for detecting system disturbances, taking into account the level of voltage at the PCC. According to the grid code, the voltage dip is classified as less severe, moderate severe and high severe based on the voltage level index given in equation (1). Depending on the severity of the fault, the FRT capability of the system is varied by controlling the reactive power of the system. Table 2 presents the fault severity level based on voltage level index with its corresponding clearing time of fault.

$$\text{Voltage level index} = \frac{\text{Actual Grid voltage}}{\text{Nominal Grid voltage}} (pu) \quad (1)$$

**B. INVERTER CONTROL STRATEGY UNDER MPPT MODE OF OPERATION**

When the system is under normal condition, it needs to be operated in MPPT mode to achieve maximum power transfer to the grid by controlling the dc-dc boost converter [21]. A fuzzy logic based MPPT is developed, to control the boost converter in which the fuzzy rule base is shown in Table 3. The input variable, E(t) is obtained from various steps of the PV slope as in equation (2), and the error is the difference between the instantaneous step ΔE(t) and previous step as in

equation (3) and the output is the duty cycle D. There are seven membership functions in the input function: Highly Negative (HN), Moderately Negative (MN), Small Negative (SN), Zero (Z), Small Positive (SP), Moderately Positive (MP), and Highly Positive (HP). The change in error (ΔE) has 3 membership functions, Negative (N), Zero (Z) and Positive (P).

The ΔE linguistic membership function is depicted using 3 linguistic functions for the fact that tuning of the limits is simple and to make sure that the tracking point on the PV graph is moving towards the MPP point. Moreover, to decrease computation time, the defuzzification method used is Center of Maximum (CoM), which is a compromise between accuracy of the FLC’s output and computation time, but it successfully produced the best results under standard test conditions. The inverter current is controlled using cross coupling strategy with double loop feed forward mechanism and is shown in Figure 2.

$$E(t) = \frac{P(t) - P(t-1)}{V(t) - V(t-1)} \quad (2)$$

$$\Delta E(t) = E(t) - E(t-1) \quad (3)$$

The voltage at the dc side of the inverter is regulated by a dc link controller and to limit the inverter current within safe limits, a proportional integral based double loop feed-forward control mechanism is implemented. A decoupling strategy is used which separates the active and reactive components of currents. The outer control loop regulates the DC link voltage to its nominal value and generate an active current reference,  $I_d^*$  as given in equation (4) along with voltage phase angle, Φ for coordinate transformation. This control ensures that under normal conditions, maximum active power transferred from solar PV system into the grid, while retaining reactive current reference,  $I_q^*$  to be 0, according to grid code compliance. The inner loop consists of PI control, with  $I_d^*$  and  $I_q^*$  as inputs and produces  $V_d^*$  and  $V_q^*$  as in equation (5 and 6) respectively. These references,  $V_d^*$  and  $V_q^*$  are transformed to  $V_{abc}$  using Inverse Parks and Clarks transformation and the inverter receives pulses from the PWM signal generator as shown in Figure 2.

$$I_d^* = k_p (V_{dc}^* - V_{dc}) + k_i \int (V_{dc}^* - V_{dc}) dt \quad (4)$$

$$V_d^* = k_p (I_d^* - i_d) + k_i \int (I_d^* - i_d) dt + \omega L_f i_q + v_d \quad (5)$$

$$V_q^* = k_p (I_q^* - i_q) + k_i \int (I_q^* - i_q) dt + \omega L_f i_d + v_q \quad (6)$$

The real power (P) and reactive power (Q) of the inverter under normal condition is given in rotating dq reference frame as follows:

$$P = \frac{3}{2} (v_d i_d + v_q i_q) \quad (7)$$

$$Q = \frac{3}{2} (-v_d i_q + v_q i_d) \quad (8)$$



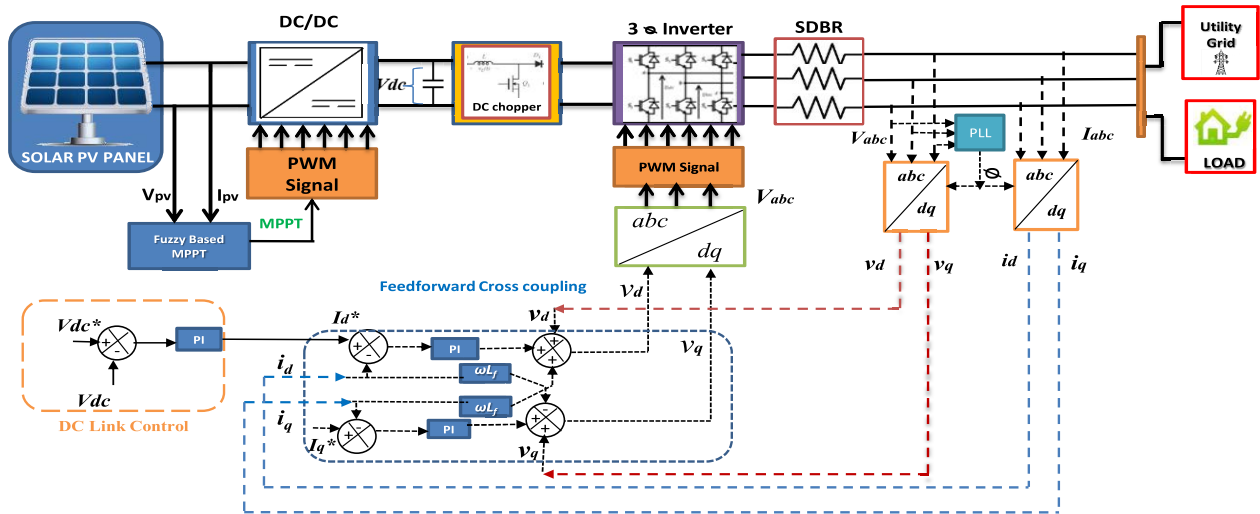


FIGURE 2. Inverter control strategy under MPPT mode of operation.

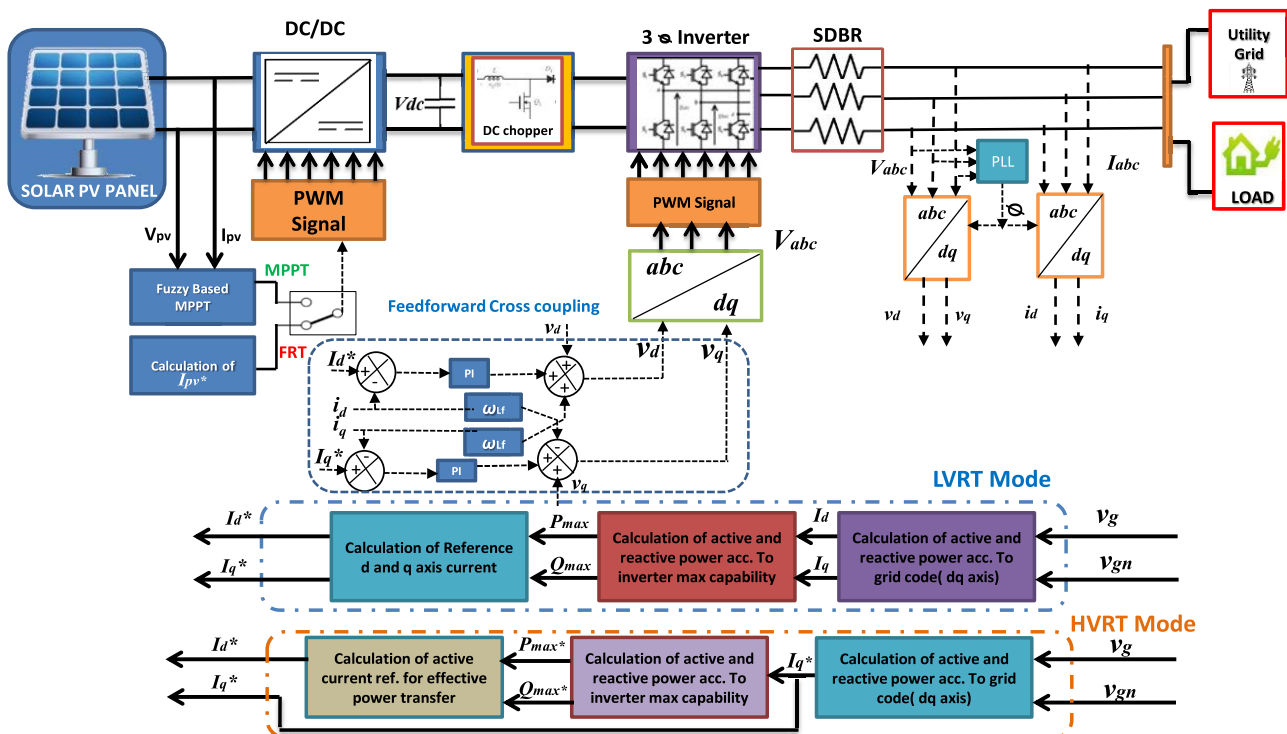


FIGURE 3. Proposed FRT Control strategy.

Neglecting  $v_q$  for a balanced system, P and Q are as follows:

$$P = \frac{3}{2} (v_d i_d) \quad (9)$$

$$Q = -\frac{3}{2} (v_d i_q) \quad (10)$$

Under normal condition as  $i_q$  is set to zero, there is no reactive power injection into the grid.

### C. INVERTER CONTROL STRATEGY UNDER LVRT MODE OF OPERATION

During grid faults, the grid voltage experiences a voltage dip and hence the real power injected into the grid is reduced and

TABLE 3. Fuzzy rule base for MPPT controller.

Error (E)	Change in Error ( $\Delta E$ )		
	Negative (N)	Zero (Z)	Positive (P)
HN	HP	MP	HP
MN	MP	SP	MP
SN	SP	Z	SP
Z	Z	Z	Z
SP	SN	Z	ZN
MP	MN	SN	MN
HP	HN	MN	HN

high current flows in the inverter side which is connected to PCC. The power imbalance at the dc side and ac side of the

inverter due to grid fault causes the input power to be greater than the output power, thereby causing an overvoltage at the dc side of the inverter. The reactive current according to the grid code is given as:

$$I_q = \begin{cases} 0, & V_g > 0.9V_{gn} \\ 2 - 2\frac{V_g}{V_{gn}}, & 0.5V_{gn} < V_g < 0.9V_{gn} \\ 1, & V_g < 0.5V_{gn} \end{cases} \quad (11)$$

where,  $V_g$  is the grid voltage during fault and  $V_{gn}$  is the grid voltage under normal conditions. The direct current  $I_d$  is calculated as

$$I_d = \sqrt{I_r^2 - I_q^2} \quad (12)$$

In this work, an improved current control based LVRT strategy is proposed in which the active and reactive currents to be injected are calculated based on the maximum power capability of the inverter. In order to get improved system performance, the proposed LVRT strategy is combined with DC chopper and Series Dynamic Braking Resistor (SDBR) which further limits the dc link voltage and over current in the inverter.

The proposed LVRT strategy is activated to achieve the following and make the GCPV remain connected to the grid:

- (1) To inject reactive current into the grid and to stabilize the grid voltage at the PCC.
- (2) To maintain dc link voltage and safeguard power converters.
- (2) To minimize the over current on the grid side of the inverter to be within the safe operating limits

The proposed LVRT strategy is combined with DC chopper and SDBR to enhance FRT capability of the system by improving the system parameters which supports grid stability as shown in Figure 3. Depending on the severity level of the fault, FRT is either fully or partially activated [22]–[24]. However, the real and reactive power injected into the grid should satisfy the following constraint:

$$\sqrt{P^2 + Q^2} < S_{max} \quad (13)$$

where P, Q are the active and reactive power injected into the grid and  $S_{max}$  is the maximum power capability of the inverter. The maximum active and reactive power transfer from inverter to the grid in the proposed LVRT control strategy during fault conditions are calculated using equation (14).

The proposed LVRT control strategy is activated during grid faults in which, the maximum range of real and reactive power capability of the inverter are computed to obtain the active and reactive current references ( $I_d^*$ ,  $I_q^*$ ) to work in LVRT mode of operation as follows:

$$P_{max} = S_{max} * \cos\left(\tan^{-1}\frac{I_q}{I_d}\right) \quad (14)$$

$$Q_{max} = \sqrt{S_{max}^2 - P_{max}^2} \quad (15)$$

$$I_d^* = \frac{2}{3} \times \frac{P_{max}}{v_d} \quad (16)$$

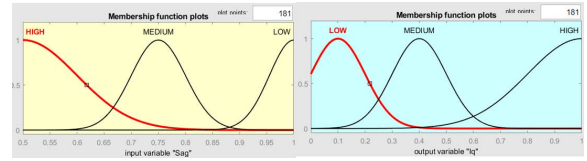


FIGURE 4. Membership functions for voltage dip and reactive current.

TABLE 4. Fuzzy rule base for improved current control based lvrt inverter strategy.

S.No.	$V_g/V_{gn}$	$I_q$
1	LOW	LOW
2	MEDIUM	MEDIUM
3	HIGH	HIGH

$$I_q^* = \frac{-2}{3} \times \frac{Q_{max}}{v_d} \quad (17)$$

During grid faults, grid stability is achieved through voltage recovery and protection of power converter systems which takes precedence than maximum power transfer. Therefore, reducing active current injection ensures reduction in inverter over current while injecting sufficient reactive current into the grid to ensure stability even during grid faults. This results in better grid stabilization and avoids voltage dip at PCC.

In the proposed LVRT control strategy, Mamdani based Fuzzy inference system is used to inject reactive power depending on the amount of calculated quadrature axis current. The fuzzy rule base is developed using the grid code to produce the quadrature axis current.

The input to the fuzzy system is the ratio of grid voltage dip ( $V_g/V_{gn}$ ), and these inputs are fuzzified into a sigmoidal membership function with three linguistic variables HIGH, MEDIUM and LOW and its range varies from 0.5 to 1. The output of the fuzzy system is the amount of reactive current to be injected into the grid. A center of gravity based defuzzification method is applied to convert a linguistic variable into a numerical output. The quadrature axis current output, is represented using a sigmoidal function with three linguistic variables high, medium and low and it ranges from 0 to 1 and the membership functions for voltage dip and reactive current is represented in Figure 4. From the fuzzy rule base given in Table 4, the reference quadrature axis current is calculated and is used to calculate the direct axis current reference using equation (11) which ensures over current reduction during grid faults without disconnection of GCPV from the grid. The computed reference currents are further fed to the feed forward controller to generate the required PWM pulses for the inverter.

During grid faults, to deliver solar power to the grid and to reduce the response time of MPPT controller after the clearance of the fault, the current reference to the boost converter has to maintain balanced power flow and is calculated as follows:

$$I_{pv}^* = I_{pv,mppt} \times \frac{V_g}{V_{gn}} \quad (18)$$

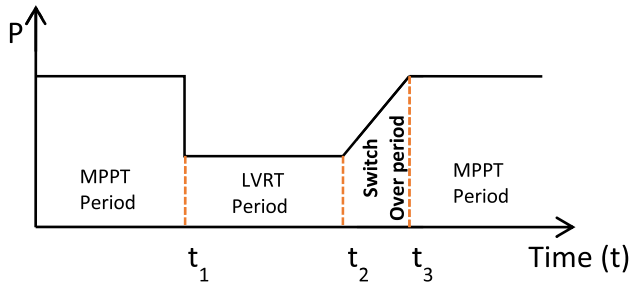


FIGURE 5. Active power response curve.

In the proposed FRT control strategy, the response curve of the active power during fault period is as shown in Figure 5. For the effective transfer between MPPT and LVRT modes of operation, the active power during the switchover period is calculated as follows:

$$P_{switchover} = (t_3 - t_2)k + P_{LVRT} \text{ for } t_2 < t < t_3 \quad (19)$$

#### D. INVERTER CONTROL STRATEGY UNDER HVRT MODE OF OPERATION

The HVRT mode of operation is activated whenever there is a rise in grid voltage above the nominal value due to sudden disconnection of the load or high reactive power compensation at PCC. In this work, analysis is carried out by disconnecting a portion of the load and is observed that the dc link voltage drops from its nominal value, increase in the grid voltage and decrease in the grid current. In HVRT mode of operation, the PV inverters are operated to absorb reactive power which leads to regulation in the voltage at the PCC. In this condition, the system is made to inject active power utilizing the maximum power capability of the inverter. The PV inverter is made to work with its full capacity which effectively absorbs reactive power. In this proposed HVRT strategy, the amount of reactive power absorbed by the GCPV system is decided by the capability of the inverter according to grid code compliance as (20), shown at the bottom of the next page. The reactive power and active power rating of the inverter  $Q_{max}^*$  and  $P_{max}^*$  to work under HVRT mode of operation is calculated using  $I_q^*$  as follows:

$$Q_{max}^* = -\frac{3}{2} (v_d I_q^*) \quad (21)$$

$$P_{max}^* = \sqrt{S_{max}^2 - Q_{ref}^{*2}} \quad (22)$$

The active current reference calculation for injection of active power during HVRT mode of operation is as follows:

$$I_d^* = \frac{2}{3} \left( \frac{P_{ref}^*}{v_d} \right) \quad (23)$$

### III. RESULTS AND DISCUSSION

The performance analysis of the proposed inverter control strategy under, MPPT, LVRT and HVRT modes of operation is tested and validated in a simulation environment of 100 kW two stage grid connected PV system in MATLAB/Simulink

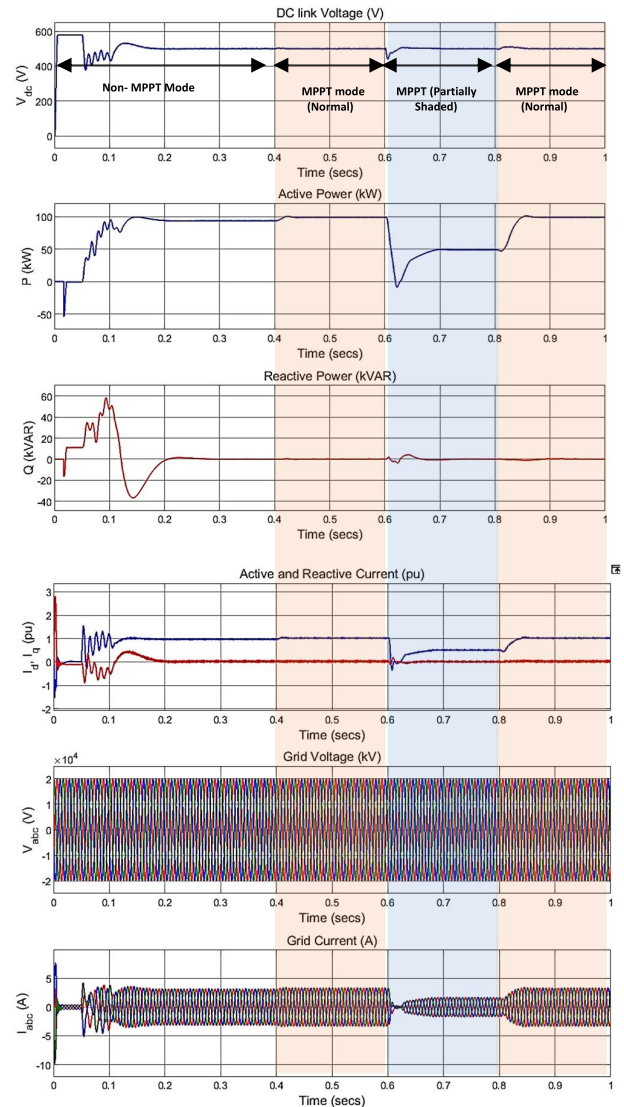


FIGURE 6. Performance analysis of 100 kW grid connected PV system under MPPT mode of operation.

2018b version and hardware experimental setup of 1 kW grid connected solar PV system.

#### A. PERFORMANCE OF PROPOSED INVERTER CONTROL STRATEGY UNDER MPPT MODE OF OPERATION

When the system is under normal conditions, fuzzy based MPPT mode of operation is activated. The specifications of 100 kW grid connected PV system is provided in Table 5. According to grid code compliance when the GCPV is in normal condition, with the fuzzy MPPT controller the current  $I_d$  is set to its maximum value and  $I_q$  is set to zero thereby ensuring maximum real power is transferred to the grid under maximum irradiance and the dc link voltage is maintained at 500V. Figure 6 depicts the system parameters under MPPT mode of operation which is investigated under different system operating conditions namely, normal irradiance and partial shaded conditions. The MPPT mode is activated at 0.4 ms and it can be observed the active power transfer from the PV

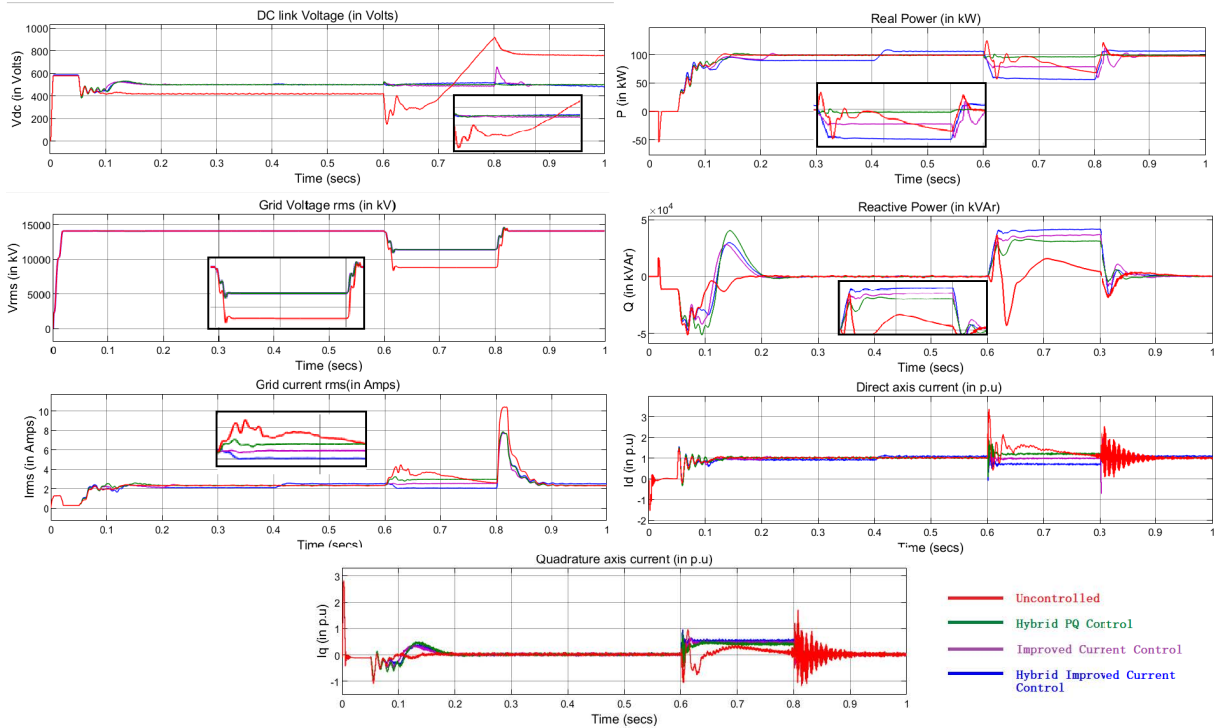


FIGURE 7. Performance analysis of 100 kW grid connected PV system under LVRT mode of operation for symmetrical fault.

TABLE 5. Fuzzy System parameter of 100 kW GCPV system.

S. No	Electrical Component	Rating
1	Solar PV Panel	100 kW ( $V_{oc}=321$ V, $I_{sc}= 393.3$ A)
2	DC-DC Boost Converter	150 kW ( $f_s=5$ kHz)
3	DC-Link Capacitor	6 mF
4	2-Level 3Φ Voltage Source Inverter	$V_{p-p}=450$ V, $f_s= 50$ Hz
5	L- Filter	250 μF
6	Step-up Transformer	260 V/ 25 kV, 25 kV/120 kV
7	Electrical Load	32 MW, 2Mvar

system to the grid is 100 kW. The proposed MPPT control scheme is also tested under partial shaded conditions (0.6-0.8 sec) which validates the generalization of MPPT controller under dynamic changing conditions.

**B. PERFORMANCE OF PROPOSED FRT CONTROL SCHEME UNDER LVRT MODE OF OPERATION**

**1) SYMMETRICAL FAULT**

The symmetrical fault is simulated in the grid side for 200ms (0.6-0.8sec). The system parameters namely, grid voltage, grid current, dc link voltage, real and reactive power are analyzed to study the performance of the proposed FRT control

strategy. It is observed that during three-phase fault, the grid current shoots and reaches 12A. Further, grid voltage drops to 9 kV from the nominal value of 20 kV and the dc link voltage shoots to very high value of 1150 V from its nominal value of 500 V.

Due to power imbalance between the dc and ac side of the inverter, the inverter does not deliver power to the faulty grid and thus the dc link voltage is increased which is harmful to the PV system and hence the PV system needs to be disconnected from the grid. According to the grid code, instead of disconnecting the PV system, the proposed FRT control strategy rides through the fault and meet the partial demand by staying connected to the grid and supports in grid stability.

The operating cycle of the dc chopper is maintained at 0% during normal conditions and 60% during grid faults. Similarly, in SDBR, the operating cycle is 95% and 0% during normal and grid faults respectively. The comparison of the system parameters using the proposed LVRT control is evaluated and compared with the other FRT strategies and is provided in Table 6 and the percentage improvement of the proposed scheme against the conventional method is provided in Table 7. The performance analysis of the proposed combined improved current controller FRT strategy is compared with the conventional PQ FRT scheme and uncontrolled case

$$I_q^* = \frac{\sqrt{I_{max}^2 - (k \times I_d)^2}}{k} \begin{cases} 1.1V_{gn} < V_g < 1.2V_{gn}, & \text{Stay connected for 2 secs} \\ 1.2V_{gn} < V_g < 1.3V_{gn}, & \text{Stay connected for 0.2 sec} \\ V_g > 1.3V_{gn}, & \text{Disconnect from grid} \end{cases} \quad (20)$$



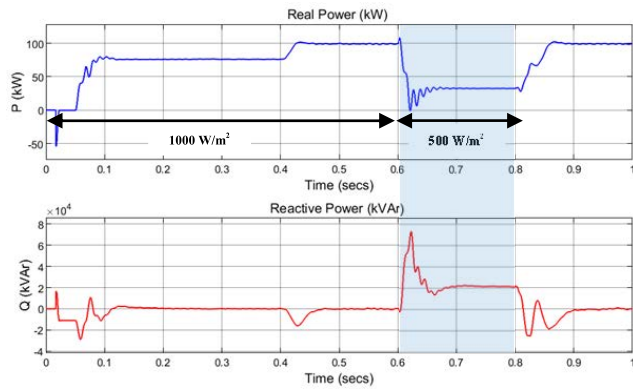


FIGURE 8. Performance analysis under varying irradiation condition.

TABLE 6. Comparison of proposed FRT strategy under symmetrical fault.

Controller	Grid Voltage RMS (kV)	Grid Current RMS (A)	DC Link Voltage (V)	Active Power (kW)	Reactive Power (kVAR)	Switch Over Period (Secs)
Without FRT Controller	9	4	1150	60	0	0.02
PQ Controller [24]	11.37	1.85	502	95.8	30.8	0.018
Improved Current Controller [25]	11.37	2.47	500	78.45	36.2	0.016
Proposed Hybrid Improved Current Controller	11.37	2	502	64	42	0.016

and is shown in Figure 7. The comparison of dc link voltage shows that it is maintained at 500 V using the proposed control strategy, with an improvement of 30% when compared to the uncontrolled case. The grid voltage during fault condition without any controller is reduced to 9 kV and in case of the proposed method, the grid voltage is maintained at 11.37 kV which shows an improvement of 23 % in the grid voltage. The active power injected into the grid from the PV has been improved to 64 kW with an improvement of 4% in comparison with the uncontrolled case. The reactive power injected into the grid is based on the level of the fault. In this case, the fault level is between 15 to 88%, the FRT mode is activated with reduced active power transfer and increased reactive power injection of 42 kVAR from the PV to the grid. It can also be noted that in the proposed FRT controller the reactive power is increased to a greater extent to stabilize the grid while maintaining the other system parameters within the limit when compared with the other FRT control schemes. The proposed FRT control is also tested under varying irradiance and dynamic load conditions under symmetrical faults by which the model is validated for all varying operating conditions enhancing the FRT capability of the system. Figure 8 represents the real power and reactive power under varying irradiation from 0.6 to 0.8 secs with an

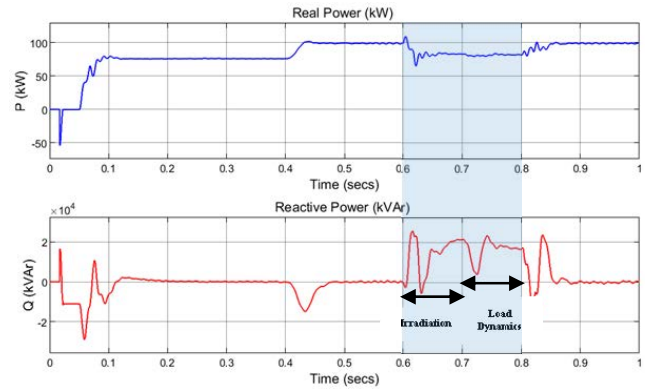


FIGURE 9. Performance analysis under dynamic loading condition.

TABLE 7. Percentage improvement of proposed FRT scheme under symmetrical fault.

SYSTEM PARAMETERS	IMPROVEMENT IN IMPROVED CURRENT CONTROLLER	IMPROVEMENT IN PROPOSED HYBRID IMPROVED CURRENT CONTROLLER
GRID VOLTAGE	23 %	23 %
GRID CURRENT	61.9 %	90.9 %
DC LINK VOLTAGE	30 %	29 %
REAL POWER	18.45 %	4 %

irradiation of 500 W/m<sup>2</sup> and Figure 9 shows the results under dynamic load condition from 0.7 to 0.8 secs.

## 2) UNSYMMETRICAL FAULT

The unsymmetrical fault (double line to ground fault) is simulated which creates the voltage dip of 15% to 80% during which the LVRT mode is activated with a sufficient amount of reactive power injection into the grid. The performance analysis of the proposed hybrid improved current control strategy in comparison with other conventional control strategies for double line to ground fault is shown in Figure 10. Table 8 depicts the uncontrolled case, and it can be noted that the grid voltage drops to 8.02 kV whereas the nominal voltage is 14 kV. The grid current is observed to be 12A where the nominal current is 2A and the dc link voltage is 920 V during double line to ground fault. With the proposed controller, the grid voltage at the PCC is improved to 11.37 kV with an improvement of 29.5 %. The inverter current is 7.6A and the improvement in grid current using the proposed control scheme is 57.8 %. The dc link voltage is brought back to its nominal value of 500 V. The active power transfer from the PV inverter to the grid is reduced to 66.4 kW and reactive power injection is increased to 55 kVAR, to support grid voltage during grid fault conditions. The percentage improvement of the proposed FRT scheme under unsymmetrical is provided in Table 9. Hence this ensures that the proposed FRT strategy is much more efficient than the other FRT schemes.

## C. PERFORMANCE ANALYSIS OF THE FRT CONTROL STRATEGY UNDER HVRT MODE OF OPERATION

The HVRT mode of operation is realized by suddenly disconnecting a portion of the load for 200ms (0.6 sec to 0.8 sec). It can be noticed that the dc link voltage drops to 390 V, the

**TABLE 8. Comparison of proposed FRT scheme under double line to ground fault.**

CONTROLLER	GRID VOLTAGE RMS (kV)	GRID CURRENT RMS (A)	DC LINK VOLTAGE (V)	ACTIVE POWER (kW)	REACTIVE POWER (kVAR)	SWITCH OVER PERIOD (SECS)
WITHOUT FRT CONTROLLER	8.02	12	920	78	0	0.18
PQ CONTROLLER[24]	11.32	7.6	502	96	43	0.3
IMPROVED CURRENT CONTROLLER[25]	11.32	8	500	73.5	48.3	0.4
PROPOSED HYBRID IMPROVED CURRENT CONTROLLER	11.37	7.6	500	66.4	55	0.18

**TABLE 9. Percentage improvement of the frt scheme under double line to ground fault.**

SYSTEM PARAMETERS	IMPROVEMENT IN IMPROVED CURRENT CONTROLLER	IMPROVEMENT IN THE PROPOSED HYBRID IMPROVED CURRENT CONTROLLER
GRID VOLTAGE	29.5 %	29.5 %
GRID CURRENT	50 %	57.8 %
DC LINK VOLTAGE	76 %	74 %
REAL POWER	6.1 %	17.4 %

real power injection is maximum and the reactive power is maintained zero. It can also be observed in the graph that, there is a rise in the grid voltage from 14 kV to 14.5 kV and the grid current reduces from 4A to 2A with ripples while reconnecting back to system. Figure 11 displays the simulation results of the system parameters with proposed FRT

controller, it can be seen that the PV absorbs reactive power during the voltage rise in grid voltage. Hence by stabilizing the grid voltage, the grid current is also maintained at its nominal value. By comparing the proposed method without any FRT scheme, it can be observed that there is a 3.5% improvement in the grid voltage, 4.7% in grid current and 78% in case of dc link voltage. The active power transfer is forced to be maintained at 100 kW and the reactive power absorbed by the inverter is 39 kVAR.

The comparison of FRT control schemes in terms of system parameters along with literature works are provided in Table 10.

**IV. EXPERIMENTAL DISCUSSION**

**A. HARDWARE DESCRIPTION**

This proposed hybrid improved current control FRT strategy is implemented in a hardware setup of 1 kW grid-tied PV system as shown in Figure 12. The configuration of hardware setup is provided in Table 11 which comprises of PV panel, boost converter, FPGA processor, inverter module, grid sensing module and 3 phase auto transformer. The grid fault is sensed by adjusting the isolation transformer for creating dip and rise in grid voltage thereby realizing the low voltage and grid voltage conditions. The proposed controllers are deployed in FPGA SPARTAN6 processor. The ac and dc side measurements are obtained from the sensors in the grid sensing module. The ac-side measurements include voltages and current at PCC and the dc-side measurements are voltage at the dc link which are acquired in the digital storage oscilloscope.

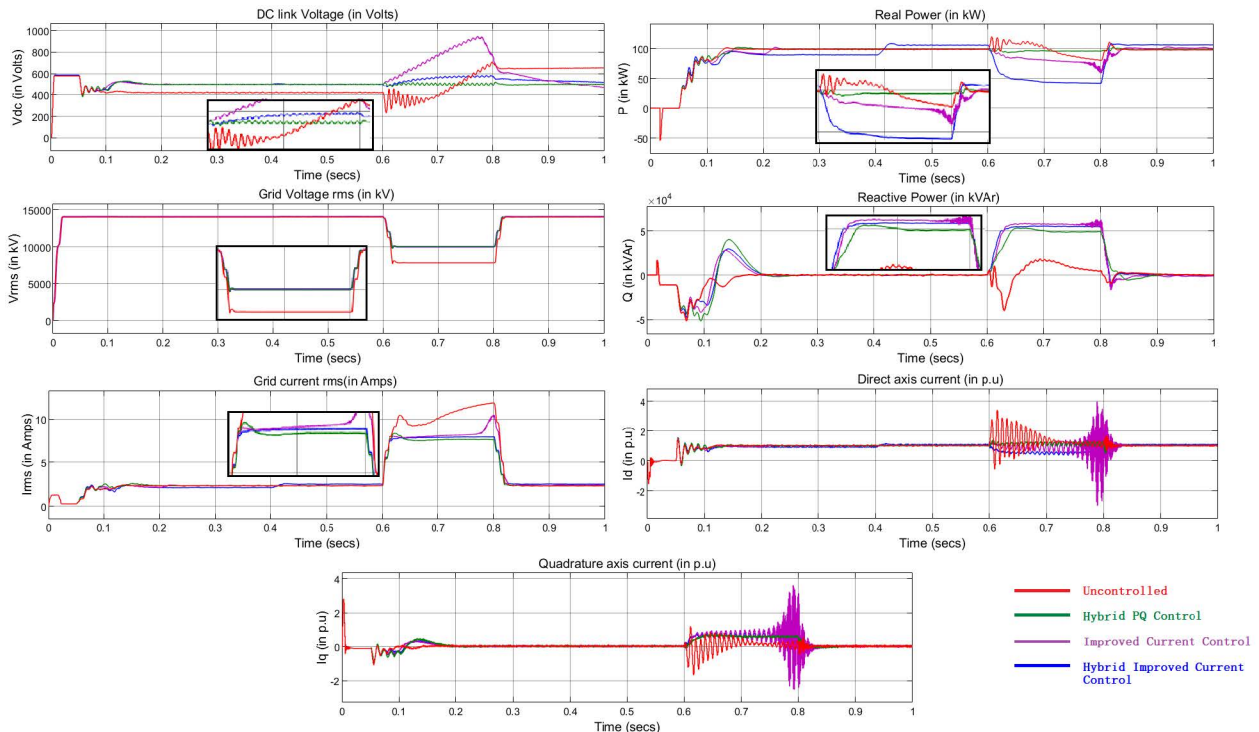


**FIGURE 10. Performance analysis of 100 kW grid connected PV system under unsymmetrical fault.**

**TABLE 10. Comparison of proposed FRT in terms of system parameters.**

Approach	Switchover Time	Peak overshoot current	Remarks
Model predictive control [26, 27]	Slow	--	Applied to different types of faults, no change in grid side over current and not tested for different faults.
Finite control set model predictive control [28]	Fast	High during voltage sag, but within the limits	Suitable for all grid codes with significant improvement in dc link voltage with initial transients in response.
Active and variable reactive power [19, 14]	Slow	High during voltage sag	Low current injection provided with reactive power support, Active and reactive powers experience oscillations
Fuzzy PQ controller [24]	Slow	High during voltage sag, but within the limits	Suitable for all grid codes with significant improvement in grid voltage, but active and reactive power experiences oscillation.
Improved current controller[25]	Fast	Within the threshold value	Suitable for all grid codes with significant improvement in grid voltage, active and reactive power.
Proposed hybrid improved current controller	Fast	Within the threshold value	Suitable for all grid codes, dc link voltage control, reactive power injection and absorption during LVRT and HVRT modes of operation

**TABLE 11. Hardware system configuration of 1 kW GCPV system.**

Parameters	Values
System Frequency	50 Hz
Line Voltage	400 V
DC-Link Voltage	218 V
Inverter Rating	5 kVA, 400 V, 10 A
DC-DC Boost Converter Rating	1.5 kW, 350 V (input), 600 V (output)
Inverter switching frequency	10 kHz
Boost converter switching frequency	5 - 20 kHz
Inverter output filter inductance	5 mH

**B. MPPT MODE OF OPERATION**

The grid connected solar PV system is analyzed under MPPT mode of operation and the output voltage and current of the boost converter is measured to be 218 V and 2.6 A respectively. Figure 13(a) displays PV voltage and PV current and Figure 13(b) represents the grid voltage and current during MPPT mode. The real power is 405 W and reactive power 0 kVAR. This indicates that during under normal system conditions the real power is maximum which depends on the irradiation as shown Figure 13(c). From the experimental results it is clear that during MPPT mode of operation the voltage and current at PCC remains constant, and maximum real power is injected into the grid maintaining reactive power to be at 0 kVAR and voltage at PCC at nominal value.

**C. LVRT MODE OF OPERATION**

Figure 10 illustrates the performance of the system parameters such as voltage at PCC, dc link voltage, grid side voltage and current after the implementation of the proposed

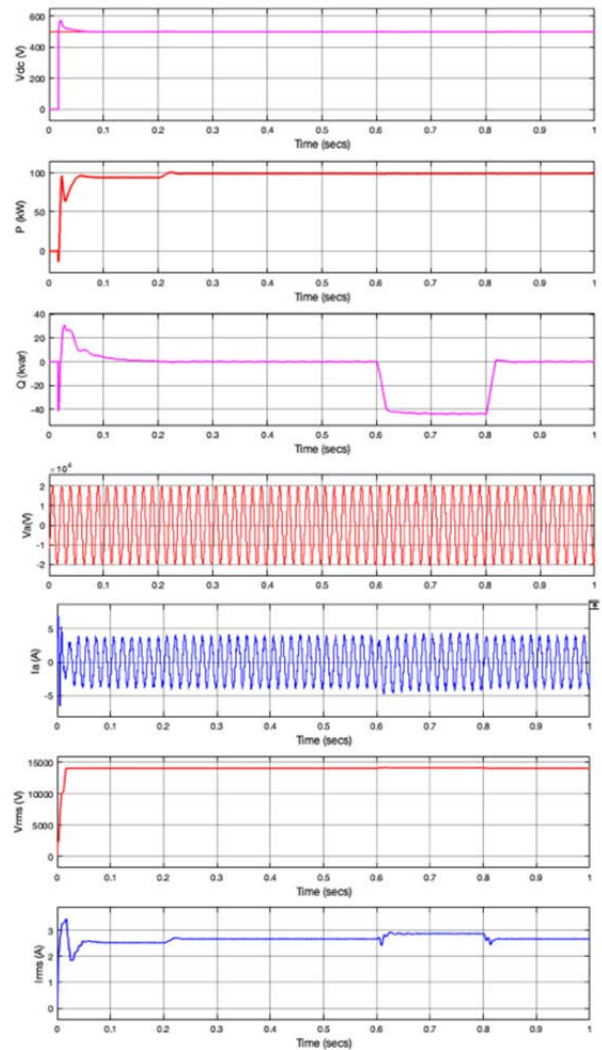


**FIGURE 11. Performance analysis of the system parameter under HVRT mode of operation.**

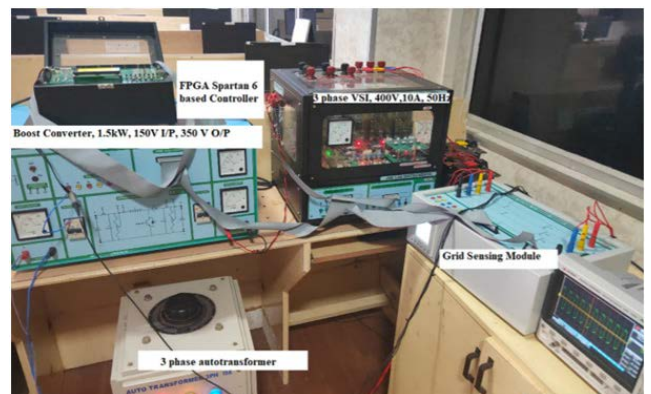


**FIGURE 12. Hardware setup of 1 kW GCPV system.**

FRT controller in FPGA Spartan6 processor. The system is analyzed for grid faults by reducing the voltage at PCC by 25 V using the isolation transformer. Using the proposed FRT controller, the inverter fed PV system injects suitable reactive power and curtails real power injection into the grid which meets the local loads partially. Figure 14 (a) shows the



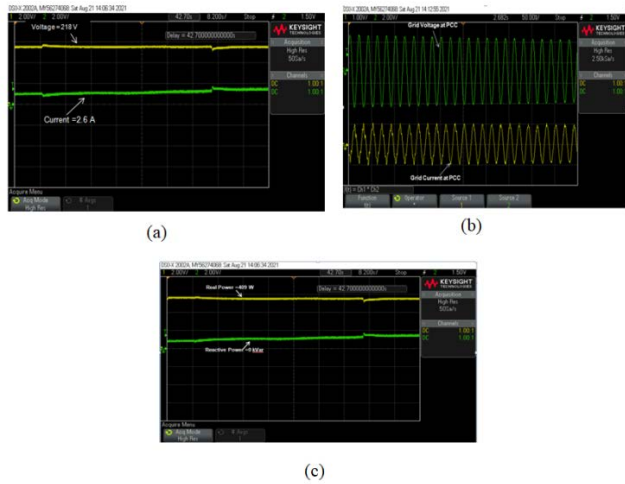


**FIGURE 13.** Performance of the real time experimental setup under MPPT mode of operation. (a) DC link voltage and solar PV current. (b) Grid voltage and current. (c) Real and reactive Power injected into the grid.

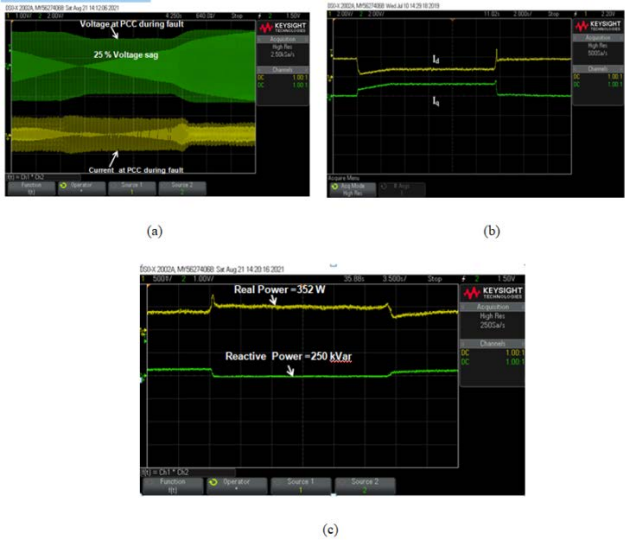


**FIGURE 14.** Performance of proposed FRT control scheme under LVRT mode of operation. (a) Voltage and current at PCC. (b) Direct and quadrature axis current. (c) Real and reactive power injected into the grid.



**FIGURE 15.** Performance of proposed FRT control scheme under HVRT mode of operation.

grid voltage and current and Figure 14(b) represents the direct ( $I_d$ ) and quadrature ( $I_q$ ) axis currents during voltage dip at PCC by 25 V. And it can be observed that the  $I_d$  is 0.05 pu and  $I_q$  is 0.3 pu. This indicates that during severe fault condition the real power reduces and reactive power injection increases in real time setup as shown in Figure 14 (c). In addition to stabilizing the grid during faults, the proposed FRT scheme satisfies the grid code requirements. Hence during grid faults,

**TABLE 12.** System parameters under inverter modes of operation in the hardware setup.

CONDITION	DC link voltage (V)	Solar PV Current (A)	Real Power (W)	Reactive Power (VAR)
MPPT Mode	218	2.6	469	0
LVRT Mode	218	2.1	536	214
HVRT Mode	218	2.1	180	424

the proposed scheme reduces the stress on the utility grid by satisfying demand while protecting power electronic components from overvoltage in the dc side and over current in the ac side of the system.

**D. HVRT MODE OF OPERATION**

The HVRT mode of operation is realized by increasing the grid voltage to 120 % of its nominal value. The nominal grid voltage is 110 V and the HVRT mode is activated when the grid voltage is 132 V in the experimental setup. And it is observed that during HVRT condition, without any FRT controller, the dc link voltage and the grid voltage rises to a high value and the grid current drops. Figure 15 shows the performance analysis of the system during HVRT mode of operation with the proposed FRT controller. It can be observed that the dc link voltage is maintained at 218 V and the real power injected into the grid is reduced by 38 % of its nominal value and the reactive power absorbed by the inverter is increased to stabilize the grid voltage at the PCC.

Table 12 gives the comparison of the different modes of operation in the hardware setup.

**V. CONCLUSION**

This paper focuses on the low voltage and high voltage ride through for a grid connected PV system. An intelligent control strategy is proposed for enhancing the low voltage and high voltage ride through schemes in grid connected PV system. Two control modes of operation namely MPPT mode and FRT mode of operation are developed to work under normal and grid fault conditions. The proposed control strategy developed as a combination of dc link controller and MPPT controller to work under MPPT mode of operation. The proposed hybrid improved current control FRT strategy combines with SDBR and braking chopper to work under FRT mode of operation. The proposed strategy works much better to improvise the system parameters like dc link voltage, real and reactive power and voltage at PCC. The proposed system is implemented and tested under both simulation environment and hardware setup. This system yields better enhancement than other FRT schemes which are validated by the test results. The proposed control strategy maintains the power balance at the point of common coupling and also keeps the grid connected throughout the fault duration and supporting in grid stability. The proposed unified model not only enhances the system parameters but also provides less transient’s during grid faults.



## REFERENCES

- [1] F. Obeidat, "A comprehensive review of future photovoltaic systems," *Sol. Energy*, vol. 163, pp. 545–551, Mar. 2018.
- [2] S. B. Kjaer, J. K. Pedersen, and F. Blaabjerg, "A review of single-phase grid-connected inverters for photovoltaic modules," *IEEE Trans. Ind. Appl.*, vol. 41, no. 5, pp. 1292–1306, Sep. 2005.
- [3] K. Fujii, N. T. Yamada, Y. Okuma, and N. Kanao, "Fault ride through capability for solar inverters," *EPE J.*, vol. 22, no. 2, pp. 30–36, Jun. 2012.
- [4] M. K. Hossain and M. H. Ali, "Low voltage ride through capability enhancement of grid connected PV system by SDBR," in *Proc. IEEE PES T&D Conf. Expo.*, Apr. 2014, pp. 1–5.
- [5] P. Singh, "Indian electricity grid code revision: Suggestions for technical requirements for wind, solar and storage," presented at the 'Expert Group Grid Code Rev.' CERC Office, New Delhi, India, Sep. 7, 2019.
- [6] M. K. Hossain and M. H. Ali, "Fuzzy logic controlled power balancing for low voltage ride-through capability enhancement of large-scale grid-connected PV plants," in *Proc. IEEE Texas Power Energy Conf. (TPEC)*, Feb. 2017, pp. 1–6.
- [7] R. Ntare, N. H. Abbasy, and K. H. M. Youssef, "Low voltage ride through control capability of a large grid connected PV system combining DC chopper and current limiting techniques," *J. Power Energy Eng.*, vol. 7, no. 1, pp. 62–79, 2019.
- [8] N. H. Saad, A. A. El-Sattar, and A. E.-A. M. Mansour, "Improved particle swarm optimization for photovoltaic system connected to the grid with low voltage ride through capability," *Renew. Energy*, vol. 85, pp. 181–194, Jan. 2016.
- [9] A. Q. Al-Shetwi and M. Z. Sujod, "Modeling and control of grid-connected photovoltaic power plant with fault ride-through capability," *J. Sol. Energy Eng.*, vol. 140, no. 2, Apr. 2018, Art. no. 021001.
- [10] Y.-S. Wu, Y.-R. Chang, C.-H. Chang, C.-W. Liu, and Y.-M. Chen, "A current control strategy for three-phase PV power system with low-voltage ride-through," in *Proc. 9th IET Int. Conf. Adv. Power Syst. Control, Oper. Manage. (APSCOM)*, 2012, pp. 1–6.
- [11] E. Radwan, M. Nour, E. Awada, and A. Baniyounes, "Fuzzy logic control for low-voltage ride-through single-phase grid-connected PV inverter," *Energies*, vol. 12, no. 24, p. 4796, Dec. 2019.
- [12] V. N. Lal and S. N. Singh, "Control and performance analysis of a single-stage utility-scale grid-connected PV system," *IEEE Syst. J.* vol. 11, no. 3, pp. 1601–1611, Sep. 2017.
- [13] A. Q. Al-Shetwi, M. Z. Sujod, and F. Blaabjerg, "Low voltage ride-through capability control for single-stage inverter-based grid-connected photovoltaic power plant," *Solar Energy*, vol. 159, pp. 665–681, Jan. 2018.
- [14] J. Miret, A. Camacho, M. Castilla, L. G. de Vicuña, and J. Matas, "Control scheme with voltage support capability for distributed generation inverters under voltage sags," *IEEE Trans. Power Electron.*, vol. 28, no. 11, pp. 5252–5262, Nov. 2013.
- [15] I. Sadeghkhani, M. E. H. Golshan, J. M. Guerrero, and A. Mehrizi-Sani, "A current limiting strategy to improve fault ride-through of inverter interfaced autonomous microgrids," *IEEE Trans. Smart Grid*, vol. 8, no. 5, pp. 2138–2148, Sep. 2017.
- [16] J. Joshi, A. K. Swami, V. Jatily, and B. Azzopardi, "A comprehensive review of control strategies to overcome challenges during LVRT in PV systems," *IEEE Access*, vol. 9, pp. 121804–121834, 2021.
- [17] M. Nasiri, A. Arzani, and J. M. Guerrero, "LVRT operation enhancement of single-stage photovoltaic power plants: An analytical approach," *IEEE Trans. Smart Grid*, vol. 12, no. 6, pp. 5020–5029, Nov. 2021.
- [18] A. Mostefa, H. M. Boulouiha, A. Allali, and M. Denai, "Mitigation of harmonics and inter-harmonics with LVRT and HVRT enhancement in grid-connected wind energy systems using genetic algorithm- optimized PWM and fuzzy adaptive PID control," *J. Renew. Sustain. Energy*, vol. 13, no. 2, Mar. 2021, Art. no. 026302.
- [19] M. Khan, A. Haque, and V. S. B. Kurukuru, "Dynamic voltage support for low-voltage ride-through operation in single-phase grid-connected photovoltaic systems," *IEEE Trans. Power Electron.*, vol. 36, no. 10, pp. 12102–12111, Oct. 2021.
- [20] A. Z. Fatama, M. A. Khan, V. S. B. Kurukuru, and A. Haque, "Hybrid algorithm for reactive power control in grid integrated photovoltaic inverters," in *Proc. Int. Conf. Power Electron., Control Automat. (ICPECA)*, Apr. 2019, pp. 1–6.
- [21] T. Radjai, L. Rahmani, S. Mekhilef, and J. P. Gaubert, "Implementation of a modified incremental conductance MPPT algorithm with direct control based on a fuzzy duty cycle change estimator using dSPACE," *Sol. Energy*, vol. 110, pp. 325–337, Dec. 2014.
- [22] S. R. Mohamed, P. A. Jeyanthi, and D. Devaraj, "Low voltage ride-through capability enhancement of grid-connected photovoltaic systems—A hybrid control approach," in *Proc. IEEE Int. Conf. Clean Energy Energy Efficient Electron. Circuit Sustain. Develop. (INCCES)*, Dec. 2019, pp. 1–6.
- [23] M. M. Hasaneen, M. A. L. Badr, and A. M. Atallah, "Control of active/reactive power and low-voltage ride through for 40 kW three-phase grid-connected single-stage PV system," *CIREC-Open Access Proc. J.*, vol. 2017, no. 1, pp. 1655–1659, Oct. 2017.
- [24] J. R. Preetha, C. P. Chandran, C. Nithya, D. Devaraj, R. Venkatesan, V. Gopal, and S. Madhura, "Design and implementation of fuzzy logic based modified real-reactive power control of inverter for low voltage ride through enhancement in grid connected solar PV system," *Control Eng. Pract.*, vol. 101, pp. 1–16, Aug. 2020.
- [25] M. Sufyan, N. A. Rahim, B. Eid, and S. R. S. Raihan, "A comprehensive review of reactive power control strategies for three phase grid connected photovoltaic systems with low voltage ride through capability," *J. Renew. Sustain. Energy*, vol. 11, no. 4, Jul. 2019, Art. no. 042701.
- [26] E. Z. Bighash, S. M. Sadeghzadeh, E. Ebrahimzadeh, and F. Blaabjerg, "Improving performance of LVRT capability in single-phase grid-tied PV inverters by a model-predictive controller," *Int. J. Electr. Power Energy Syst.*, vol. 98, pp. 176–188, Jun. 2018.
- [27] F. Diaz-Franco, T. Vu, T. E. Mezyani, and C. S. Edrington, "Low-voltage ride-through for PV systems using model predictive control approach," in *Proc. North Amer. Power Symp. (NAPS)*, Sep. 2016, pp. 1–6.
- [28] M. A. Khan, A. Haque, V. S. B. Kurukuru, and S. Mekhilef, "Advanced control strategy with voltage sag classification for single-phase grid-connected photovoltaic system," *IEEE J. Emerg. Sel. Topics Ind. Electron.*, vol. 3, no. 2, pp. 258–269, Apr. 2022.



**C. NITHYA** (Member, IEEE) received the B.E. degree in electrical and electronics engineering from the BMS Institute of Science and Technology and the M.Tech. degree from SRM University. She is currently pursuing the Ph.D. degree with the SRM Institute of Science and Technology, where she holds the position of an Assistant Professor with the Department of EEE. Her research interests include voltage stability and grid integration issues of renewable energy.



**J. PREETHA ROSELYN** (Senior Member, IEEE) received the B.E. degree in electrical and electronics engineering from Madras University, the M.S. degree (by research) from Anna University, and the Ph.D. degree from the SRM Institute of Science and Technology. She is currently a Professor with the Department of EEE, SRM Institute of Science and Technology, and a Faculty Mentor of the SRM MTS students chapter. She has published 42 articles in international journals, 31 papers in international conferences, five lecture notes, and one book. Her research interests include voltage stability, soft computing applications in power systems, grid integration issues of renewable energy, and smart metering infrastructure.